Effects of Nanosilica Particles and Randomly Distributed Fibers on the Ultrasonic Pulse Velocity and Mechanical Properties of Cemented Sand

Saman Soleimani Kutanaei, Ph.D.[1]; and Asskar Janalizadeh Choobbasti[2]

Abstract: Randomly distributed fiber and cement can be used for various purposes. However, no attention has been paid to the use of randomly distributed fiber and cement on seismic wave velocity of sandy soil and the relation between seismic wave velocity and unconfined compressive strength. In addition, there is no previous report on the use of nanosilica particles as a modifier for fiber-reinforced cemented sandy soil. In this study a series of unconfined compression tests and 144 ultrasonic pulse velocity tests have been conducted to explore the effects of polyvinyl alcohol (PVA) fiber and nanosilica particles on the mechanical characteristics of cemented sandy soil. Moreover, microstructural properties of cemented sand with nanoparticles have been investigated using scanning electron microscope, atomic force microscopy, and X-ray diffraction test. Finally, the ultrasonic pulse velocity test for the specimens has been performed in order to estimate the unconfined compression strength of fiber-reinforced cemented sand with nanosilica. The results of this study show that the inclusion of randomly distributed fiber increases the energy absorption capacity. Moreover, the secant modulus of elasticity of a specimen decreased with the increase of fiber content. Based on the results, a correlation between pulse ultrasonic velocity and the unconfined compressive strength at different ages was proposed. **DOI: 10.1061/(ASCE)MT.1943-5533.0001761.**

Author keywords: Cement; Nanosilica; Unconfined compressive strength; Fiber; Ultrasonic pulse velocity.

Introduction

The stabilization of local soils with additive cement agents for the construction of canal lining, foundations, and pavement bases presents great environmental and economic benefits, avoiding the use of borrowed materials. Stabilization improves durability and soil strength, reduces cost and dust in the work environment, conserves aggregate materials, improves soil workability, helps reduce soil (fine grain) volume change (contraction and expansion) due to moisture or temperature, and waterproofs the soil. Cementation plays a significant role in the behavior of soils under applied loads, and has been investigated extensively around the world. However, the inclusion of cement agents in soil results in a brittle response that can be controlled by the application of randomly distributed fibers (Choobbasti et al. 2014; Kutanaei and Choobbasti 2015a). Ateş (2016) explored the use of glass fiber–cement as reinforcement to improve the mechanical characteristics properties of sand. The results showed that the addition of portland cement leads to the reduction of displacement at failure index and ductility. Moreover, the utilization of cement increased the stiffness and unconfined compressive strength noticeably.

Mechanical properties of cemented sandy soils have been widely studied (Clough et al. 1981; Consoli et al. 2000). In particular, in case of using cement-stabilized soils at a shallow depth, the degree of brittle response may be more pronounced due to a low confining pressure. Adding discrete fiber to soil can provide a reinforcement mechanism by developing tensile forces that contribute to the stability of the soil-fibers composite. Several researchers have attempted to explore the impact of randomly distributed fiber on granular and clayey soils. These studies showed that fiber reinforcement has its unique advantages. For example, friction between fiber and soil particles increases the bonding between the particles of soils and this can increase failure stress, failure strain, and the peak and ultimate strength of soils (Consoli et al. 2012; Maher and Ho 1993; Tang et al. 2007). Tang et al. (2016) examined the effect of fiber contents (FCs), water content, and dry density on the tensile strength of fiber-reinforced soil. The results showed that the tensile strength of both unreinforced and reinforced samples increased with increasing dry density and decreased with increasing water content. In addition, the surface crack reduction ratio increased with increasing the percentage of fiber.

Consoli et al. (2004) explored the impact of polypropylene (PP) and polyester (PE) fibers on the mechanical properties of cement-stabilized soils. They found that the addition of polypropylene fiber significantly improved the brittle response of cement-stabilized soils, whereas the deviatoric stresses at failure slightly decreased. Tang et al. (2007) studied the impact of fiber and cement inclusion on behavior of clayey soils. Consoli et al. (2010) conducted triaxial compression tests to explore the effect of fiber reinforcement on the mechanical properties of sand. They proposed polynomial equations to determine residual and peak strength based on percentage of fiber, cement content, and confining stress. Dehghan and Hamidi (2016) investigated triaxial shear response of cemented gravelly sand reinforced with discrete fiber. They founded that the effect of fiber on triaxial shear strength of cemented gravelly sand decreased with the increase in percentage of gravel. Kutanaei and Choobbasti (2015b) conducted a series of unconfined compressive tests in order to present an empirical equation for prediction of mechanical behavior of fiber-reinforced cemented sandy soil.

[1]Ph.D. Candidate, Dept. of Civil Engineering, Babol Univ. of Technology, P.O. Box 484, 4714871167 Babol, Iran (corresponding author). E-mail: samansoleimani16@yahoo.com

[2]Associate Professor, Dept. of Civil Engineering, Babol Univ. of Technology, P.O. Box 484, 4714871167 Babol, Iran.

Note. This manuscript was submitted on March 11, 2016; approved on July 26, 2016; published online on September 27, 2016. Discussion period open until February 27, 2017; separate discussions must be submitted for individual papers. This paper is part of the ***Journal of Materials in Civil Engineering***, © ASCE, ISSN 0899-1561.

A nanoparticle is defined as a particle that has at least one dimension at the nanometer scale (Tavakoli et al. 2014a, b). Luo et al. (2012) performed several unconfined compressive, swell potential, and California bearing ratio tests in order to investigate the mechanical characteristics of cohesive soils with sewage sludge ash stabilized with cement and nano aluminum oxide. They concluded that the unconfined compressive strength and California bearing ratio increases and swell potential decreases with an increase in nano aluminum oxide content. Taha (2009) explored the effect of nanosoil obtained from ball mill operations on Atterberg limits and unconfined compressive strength of cemented soil. The results indicated that the presence of nanosoil resulted in a significant increase in unconfined compressive strength of cement-stabilized soil and a reduction in Atterberg limits. Bahmani et al. (2014) studied the impact of nanosilica particles on the hydraulic conductivity, Atterberg limits, and compressive strength of cement-stabilized residual soil. Their results showed that addition of nanosilica leads to the reduction of plasticity index and hydraulic conductivity. Ghasabkolaei et al. (2016) explored the use of nanoparticles to improve geotechnical properties of cemented clay. They indicated that adding 1.5% nanosilica improved the unconfined compressive strength of the cemented clay up to 38% at 28 days curing. Previous studies also showed the effectiveness of nanosilica inclusions when it is mixed with cement-based material due to their high activity, accelerating cement hydration (Kutanaei and Choobbasti 2016; Choobbasti et al. 2015).

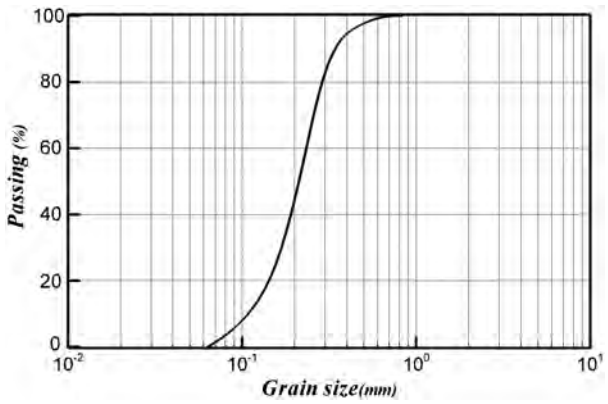

Fig. 1. Particle size distribution

Research Significance

Behavior of fiber-reinforced cemented sandy soil has been widely studied. However, no attention has been paid to the use of randomly distributed fiber and cement agenton seismic wave velocity of sandy soil and relation between seismic wave velocity and unconfined compressive strength. Although nanoparticles can be used for various purposes, no attention has been paid to the use of nanoparticles as a modifier for fiber-reinforced cemented sandy soil. Moreover, to the best knowledge of the authors, the combined effects of nanosilica and fibers on the seismic wave velocity of soil has not been studied yet. The main objective of the present study is to evaluate the combined effects of fibers and nanosilica on the mechanical properties of cemented sand. Unconfined compressive strength and ultrasonic pulse velocity tests were performed and the effect of these variables on the results is investigated. Moreover, microstructural properties of cemented sand with nanoparticles were assessed using atomic force microscopy, scanning electron microscope (SEM), and X-ray diffraction (XRD).

Experimental Program

One hundred forty-four unconfined compression tests, 144 ultrasonic pulse velocity tests, six SEM tests, and two XRD test were performed to investigate the effects of nanosilica and polyvinyl alcohol (PVA) fiber on the performance of cemented sand.

Materials

Babolsar fine-grained sand was used in this study. The particle size distribution curves for Babolsar sand are shown in Fig. 1. A SEM image of Babolsar sand particles is presented in Fig. 2(a). The cement agent used in the study was ordinary portland cement Type II. The chemical and physical properties of cement are shown in Tables 1 and 2. In this study, amorphous nanosilica with a solid content of more than 99% is used. Physical properties of nanosilica particles are presented in Table 3. A SEM image of nanosilica particles is shown in Fig. 2(b). PVA fibers 0.1 mm in diameter

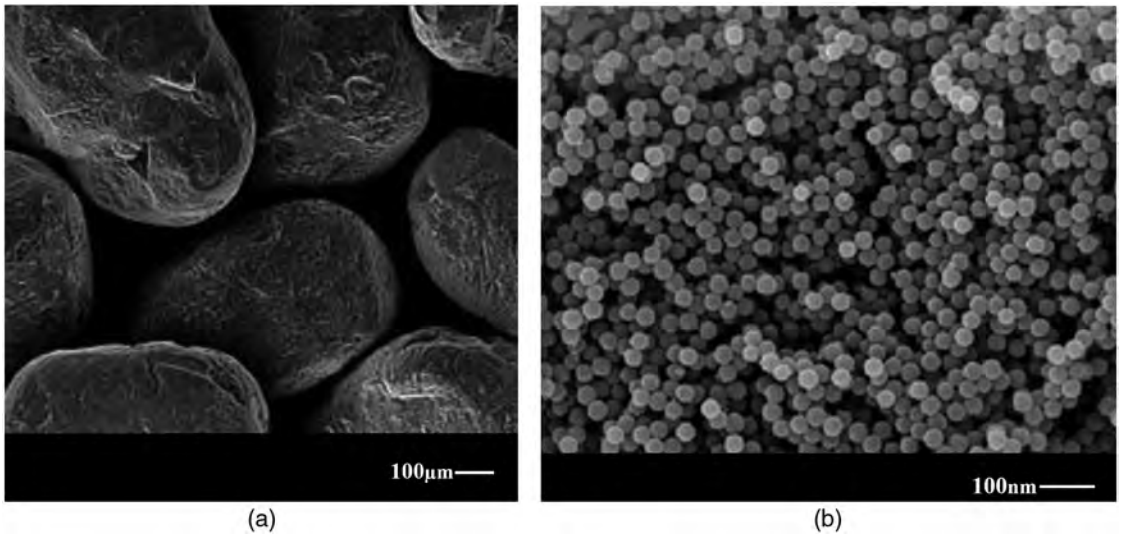

Fig. 2. SEM images: (a) sand; (b) nanosilica

Table 1. Chemical Compositions of Cement

Oxide	Percentage by weight (%)
SiO_2	21.90
Al_2O_3	4.86
Fe_2O_3	3.30
CaO	63.33
MgO	1.15
SO_3	2.10
$CaCO_3$	—
LOI	2.40

Table 2. Analysis of Physical Properties of Cement

Property	Value
Blaine (cm^2/g)	3,050
Expansion (autoclave) (%)	0.05
Specific gravity	3.1
Compressive strength (kg/cm^2)	
3 days	185
7 days	295
28 days	397

Table 3. Physical Properties of Nanosilica

Property	Value
Diameter (nm)	20–40
Surface volume ratio (m^2/g)	193
Density (g/cm^3)	1.7
Purity (%)	>99
Shape	White powder

Table 4. Properties of PVA Fiber

Property	Value
Specific gravity	1.3
Cut length (mm)	12
Diameter (mm)	0.1
Tensile strength (MPa)	1,078
Young's modulus (MPa)	25,000
Melting point (°C)	225
Water absorption	<1% by weight

and 12 mm in length are used in research. The properties of the PVA fibers are presented in Table 4. Distilled water was used for specimen preparation.

Specimen Preparation

The undercompaction technique was used for specimen preparation in this study based on the method described by Ladd (1978). The requisite amount of oven-dried sand was mixed with the desired amount of portland cement, nanosilica, and an optimum water content. During the specimen preparation, it was important to add the water prior to adding the randomly distributed fibers to prevent floating of the fibers. Fiber was then added and mixed using an electric mixer. After the mixing process, the mixture was divided into five portions and stored in a covered container to avoid moisture losses before compaction. Each portion was transferred into a 52-mm diameter by 104-mm high split mold and compacted using a metal hammer until the desired height was reached. The top

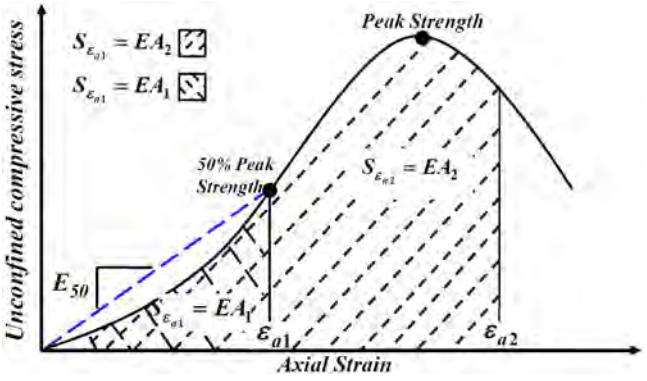

Fig. 3. Energy absorption capacity and modulus of elasticity in unconfined compression test

of each layer was scratched before adding the next layer to promote suitable bonding. The tests were conducted on the specimens with relative density of 80%. Each specimen was extracted from the split mold and was cured in a humid room at a constant temperature of 25 ± 2°C and >90% relative humidity for 7, 28, and 90 days. Before tests, the samples were submerged in distilled water for 1 day (24 h) for saturation to minimize matric suction. The water temperature was controlled at a constant temperature of 25 ± 2°C. Immediately before the unconfined compressive test and ultrasonic pulse velocity test, the samples were removed from the water container and dried with an absorbent cloth.

Results and Discussion

Matric Suction

The process of submerging the samples for 1 day (24 h) before the unconfined compression tests was satisfactory to ensure a repeatable and high degree of saturation. The matric suction (capillary forces) measurements were conducted on specimens after failure in the unconfined compression tests. The matric suction was measured in accordance with ASTM D5298 (ASTM 2010a) using the filter paper method. All the samples were tested in an unsaturated condition and a certain level of suction might be presented. Matric suction measurements were performed on certain samples. The matric suction values ranging from about 0.8 to 4.6% of the unconfined compressive strength (11–230 kPa). Given the small values of matric suction (capillary forces) measured in these samples, the small impact on unconfined compressive strength arising from the unsaturated nature was disregarded.

Secant Modulus of Elasticity and Energy Absorption Capacity

Unconfined compression tests were performed in accordance with the ASTM D2166 (ASTM 2010b) test method. The samples were loaded at a displacement rate of 1 mm/min. The secant modulus of elasticity (E_{50}) was calculated from one-half of the axial strain at peak strength (Fig. 3). Energy absorption capacity (EA) can be determined by calculating the area below the axial stress–axial strain curve (Fig. 3). To assess the validity of the obtained results, two samples prepared from each mixing design and tested. After each test, the average error was calculated. The test results were considered suitable for presenting if their average error was less than 5%.

Fig. 4 shows the variation of E_{50} with fiber content at different nanosiliaca content for specimens containing 4% cement. As seen in this figure, adding fibers to the specimens reduces the secant modulus of elasticity. This behavior can be explained by the fact that randomly distributed fibers require an initial deformation to begin strength mobilization, which results in the reduction of fiber-reinforced cemented soil stiffness. The variation of secant modulus of elasticity with the nanosilica content (NC) is also shown in Fig. 4, which shows that an increase in nanosilica up to 8% increased the secant modulus of elasticity in all specimens. The reason can be inferred to be the higher density of the cement part of the specimen, especially in the transmission zone due to the higher proportion of nanosilica. But by adding more nanosilica, the secant modulus of elasticity decreases.

Fig. 5 shows the variation of energy absorption capacity by FC at different axial strains for samples with 4% cement and different NC after 7 days curing. As can be seen in Fig. 5, at low strain the energy absorption capacity for a specimen with low percentages of fiber is greater than that of a specimen with high percentages of fiber. But at high strain, energy absorption capacity for a specimen with high percentages of fiber is greater than that of a specimen with low percentages of fiber. Moreover, Fig. 5 indicates that in all specimens, when nanosilica content increased to an optimum value of 8% in the specimen, energy absorption capacity of the samples was enhanced.

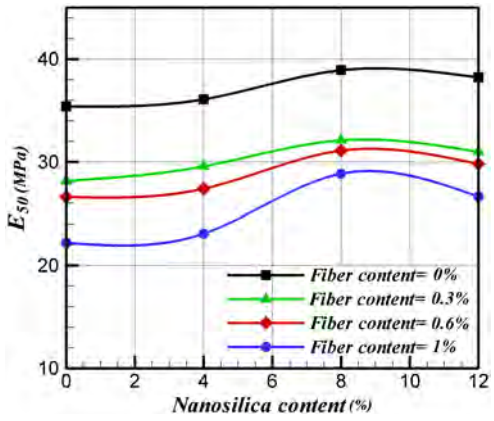

Fig. 4. Secant elastic modulus, E_{50}, of fiber-reinforced cemented specimen with different fiber contents and nanosilica contents for 7 days curing

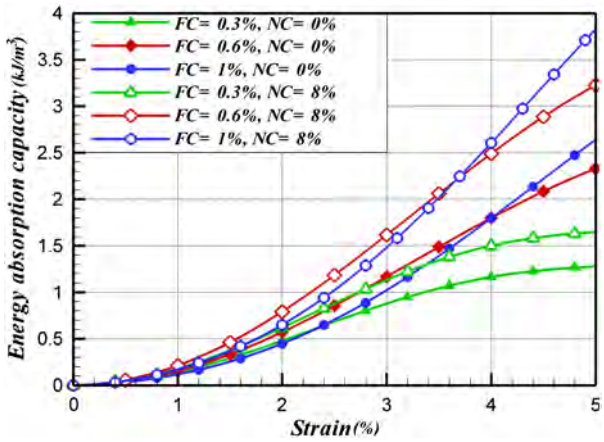

Fig. 5. Variation of the absorbed energy with axial strain for different fiber for 7 days curing

Mechanical properties improvement due to nanosilica increase up to 8% can be attributed to the following mechanisms:

1. Pozzolanic reaction: A large amount of calcium hydroxide [$Ca(OH)_2$] crystals is produced during the cement particles–water reaction [Eqs. (1) and (2)]. Crystals of calcium hydroxide were harmful for mechanical properties. Nanoparticles, due to their high specific surface area (SSA) and reactive attribute, produce calcium silicate hydrate (C-S-H) gel as a result of reaction with calcium hydroxide. Calcium silicate hydrate gel fills the pores to give the cement soil a denser structure and improves the binding of the matrix. Therefore, the compact calcium silicate hydrate gel is produced, while a pozzolanic reaction prevented more growth of crystals of calcium hydroxide [Eq. (3)]. The density of transition zone increases by filling pores and thus improves the mechanical properties (Beigi et al. 2013; Li 2004)

$$2C_3S + 11H_2O \rightarrow C - S - H + 3Ca(OH)_2 \quad (1)$$

$$2C_3S + 9H_2O \rightarrow C - S - H + Ca(OH)_2 \quad (2)$$

$$2SiO_2 + 3Ca(OH)_2 \rightarrow 3CaO \cdot 2SiO_2 \cdot H_2O \quad (3)$$

2. Nanofilling impact: Calcium silicate hydrate gel constitutes 70% of hydration productions. The average diameter of particles of calcium silicate hydrate gel is approximately 10 nm. Nanosilica, having filling ability, fills the pores in calcium silicate hydrate gel and makes a condensed adhesive cement matrix (Li et al. 2006).
3. Nucleus effect: When a low percentage of nanosilica was homogenously dispersed in the cement paste matrix, the nanosilica acted like the nucleus forming as a result of their very high specific surface area and very high surface energy. Thus, the hydration trend continued and mechanical properties of the sample are expected to improve (Li et al. 2005; Bahadori and Hosseini 2012).
4. Controlled crystallization: When the percentage of nanoparticles and the distance between nanosilica particles are appropriate (uniform spacing among particles), the crystallization will be controlled to produce a suitable state by restricting the formation and growth of calcium hydroxide crystals. This makes the cement paste matrix more uniform, compact, and homogeneous (Bahadori and Hosseini 2012).

The mechanical properties of the nanosilica samples decrease with the increase of percentage of nanosilica from 8 to 12%. There are two mechanisms for the reduction in mechanical properties when increasing nanosilica particles more than the optimum percentage. Nanosilica particles have high specific surface area; hence, they are likely to form unstable structure and weak zones in a specimen, which decreases the mechanical properties of specimens. Moreover, increasing the percentage of nanosilica restrains the suitable formation process of calcium hydroxide crystals in the transition zone and the cement matrix mechanical properties decrease. If calcium hydroxide crystals do not have sufficient growth, a pozzolanic reaction would not occur and thus cracks appear in the structure of the sample and the mechanical properties would not have suitable improvement (Beigi et al. 2013; Li et al. 2006; Choobbasti et al. 2015).

Ultrasonic Pulse Velocity

Seismic wave velocity depends on many parameters such as type of the cement, specimen age, and specimen length. A nondestructive test was performed on the samples at the age of 7, 28, and 90 days for specimens that have 2, 4, and 6% cement content and different nanosilica and fiber content. Frequencies of transmission pulses were 50 kHz and travel time was obtained at the microsecond level and is shown on a digital screen with resolution up to 0.01μs. Calculating the travel time for the ultrasonic pulses and considering the specimen length (104 mm), ultrasonic pulse velocity can be calculated by using the following formula:

$$V = \frac{L}{T} \tag{4}$$

where L = distance of propagation of the ultrasonic pulse (km); T = travel time in the specimen; and V = ultrasonic pulse velocity in the specimen. The effect of percentage of cement and curing time on ultrasonic pulse velocity of cemented sand is shown in Fig. 6. The figure reveals that the ultrasonic pulse velocity increases with increasing the percentage of cement and curing time. As the curing progresses, reactions occur between the sand particles and the cement particles. These reactions generally result in an increase in the stiffness of the cement-treated sand. The ultrasonic pulse velocity increases with increased stiffness of the cement-treated sand. The increase in ultrasonic pulse velocity of cemented can be explained by three reasons:

1. In general, a higher of percentage of cement in the cemented sand results in greater heat development, accelerating the strengthening and hydration processes. Cement particles were apparently the primary bonding agent in the cement-treated sand mixture, where cement hydration formed a stiffer soil matrix in the treated samples.
2. The beneficial impact of an increase in interparticle contacts (ultrasonic pulse path) in the cement-treated soil has been explored by several researchers. Chang and Woods (1992) performed a series of electron microscopy tests on different treated soils with various kinds of cement agent. They indicated that the mechanism by which the decrease in porosity of mixture influences the unconfined compressive cement strength of cement-treated sand is related to the existence of a larger number of interparticle contacts (ultrasonic pulse path). Hence, the specimen with a high percentage of cement has higher ultrasonic pulse velocity and unconfined compressive strength.
3. The inclusion of cement led to a higher density and denser structure, thus providing a suitable wave traveling path. To explore the impacts of cement content on the maximum dry density of cement treated sand, standard Proctor compaction tests were done in accordance with ASTM D698 (ASTM 2010c). A series of standard Proctor tests were conducted for the sand specimens containing different percentages of cement. Results on dry unit weight versus water content for sand and cement treated are presented in Fig. 7. It can be seen that the maximum dry density of the cement-treated sand increases with the increase in percentage of portland cement. This result can be explained by two reasons. Cement particles have a higher specific gravity (3.1) than sand particles (2.78), which results in increasing the maximum dry density when added to soil. On the other hand, cement has finer grains than sandy soil; hence, the pore within the coarse aggregate becomes occupied by cement particles and makes a coherent and dense structure with higher maximum dry density.

The influence of nanosilica content on the ultrasonic pulse velocity and unconfined compressive strength at the age of 2, 7, 28, and 90 days is shown in Fig. 8. The figure shows that the ultrasonic pulse velocity increases with increasing nanosilica content. The reason can be referred to the higher density of the cement part of the specimen due to the higher proportion of nanosilica. The cement part of the specimen is less able to transmit the ultrasonic pulses; hence, reduced pores and microcracks cause higher velocity. It can be also seen that the unconfined compressive strength and ultrasonic pulse velocity increase with increase of the curing time. The reason can be inferred to be the elimination of microcracks in the cement part of the specimen and hydration development when the samples get older. The curve slope decreases with increasing nanosilica content, which indicates that increasing nanosilica content causes specimens to have a faster ultrasonic pulse velocity and unconfined compressive strength.

To further explain the rapid pozzolanic reaction of nanosilica particles, it can be said that for nanoparticles with unsaturated bonds the pozzolanic reaction process between nanosilica is as follows:

$$\equiv \mathrm{Si} - \mathrm{O} - + \mathrm{H} - \mathrm{OH} \rightarrow \equiv \mathrm{Si} - \mathrm{OH} \tag{5}$$

$$\equiv \mathrm{Si} - + \mathrm{H} - \mathrm{OH} \rightarrow \equiv \mathrm{Si} - \mathrm{OH} \tag{6}$$

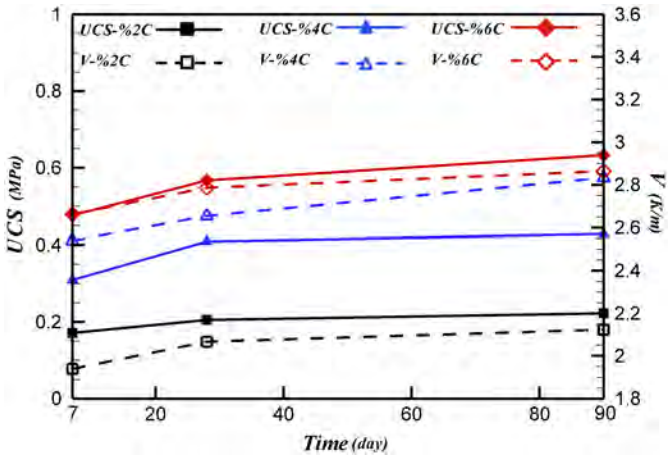

Fig. 6. Effect of curing time and cement content on ultrasonic pulse velocity and unconfined compressive strength for specimen without fiber

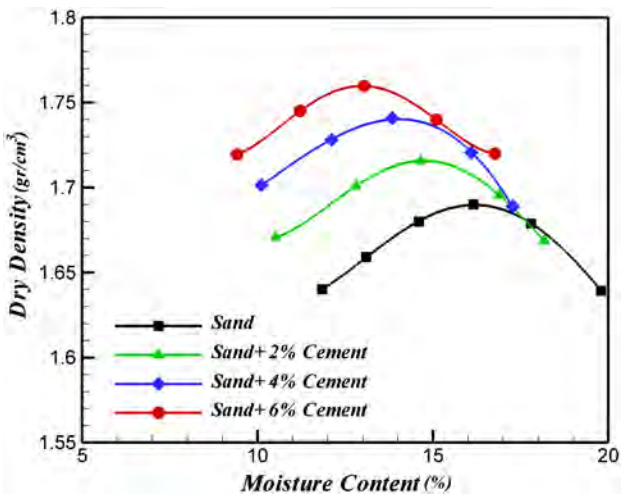

Fig. 7. Standard compaction curve

$$\equiv Si - OH + Ca(OH)_2 \rightarrow C - S - H \quad (7)$$

Thus nanosilica particles undergo pozzolanic quick reactions. By decreasing the size of materials to nanoparticle, many atomic uneven degrees are made which amplify the chemical reaction. Hence, nanosilica particles have very high surface energy, which causes atoms (nanosilica) to react with other external atoms (hydrated cement) and therefore enhances pozzolanic activity of nanosilica at low curing times.

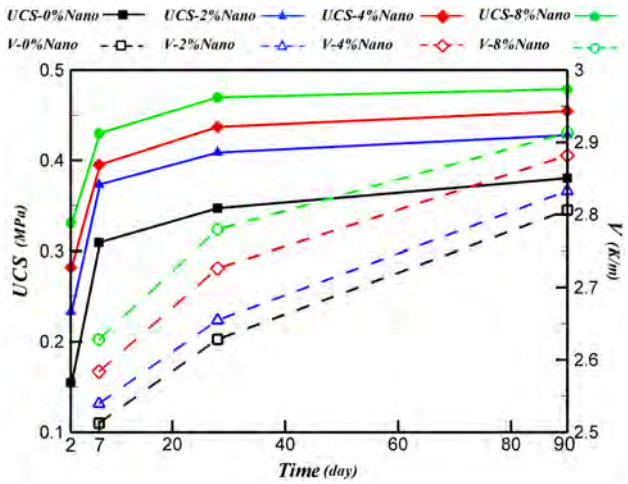

Fig. 8. Effect of curing time and nanosilica content on ultrasonic pulse velocity and unconfined compressive strength for specimen without fiber (cement content = 4%)

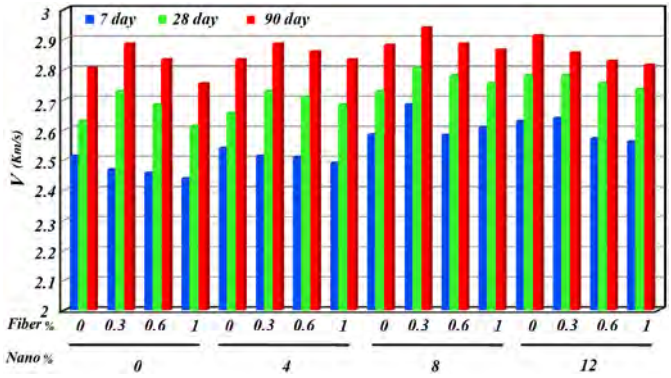

Fig. 9. Influence of the specimen age, nanosilica content, and fiber content on ultrasonic pulse velocity for samples with 4% cement

Fig. 9 shows the effect of fiber content, nanosilica content, and curing time on the ultrasonic pulse velocity for samples with 4% cement. As can be seen, inclusion of 0.3% fiber increases the ultrasonic pulse velocity in almost all of the samples for all of the curing times, but adding more fiber (0.6 and 1%) decreases the ultrasonic velocity, so the maximum ultrasonic pulse velocity is 2.88 km/s for the 90-day-old sample with 0.3% fiber added while it is 2.8 km/s for the sample without fiber at the same curing time (for specimens without nanosilica). For low fiber specimens (up to 0.3%), the inclusion of fibers would fill some of the pores in the cement-sand-matrix, thus providing a suitable wave travelling path. However, the further inclusion of fibers beyond 0.3% resulted in a decrease of ultrasonic pulse velocity. This behavior is explained by the fact that the addition of fibers to the cement-sand mixture decreases density. Moreover, the addition of a softer material (fibers) to the cement-sand mixture creates softer ways along the ultrasonic pulse path.

SEM photos were used to investigate the homogeneity and distribution of the fibers in the cement-sand-matrix before testing. SEM images obtained from cut-up sections of fiber-reinforced cemented sand with 6% cement and 0.6% fiber and cement-treated sand with 6% cement are presented in Fig. 10. The SEM images were taken after curing. It can be seen that in the cemented sand specimen, the sand grains are well coated by the cement particles. Fig. 10(b) shows that for fiber-reinforced cemented sand, although prior to the specimen preparation, the mixing was continued until achieving a uniform fiber distribution throughout the entire cemented sand specimen. However, the SEM photo from the fiber-reinforced cemented sand specimen reveals that at microscale, the homogeneity is not as good as observed in the visual inspection. Hence, the addition of randomly distributed fibers to the cement-stabilized sand decreases homogeneity and traps the traveling wave. Moreover, from the SEM photo obtained from the reinforced cement-stabilized sand sample, it can be seen that the fibers have a preferred near-horizontal orientation in the cement-sand-matrix, which is not surprising considering the process of fabrication of the samples moist tamping during which a static pressure is applied along the longitudinal axis of the fiber-reinforced cemented sand sample. Wood et al. (2007) and Ibraim et al. (2012) reported that

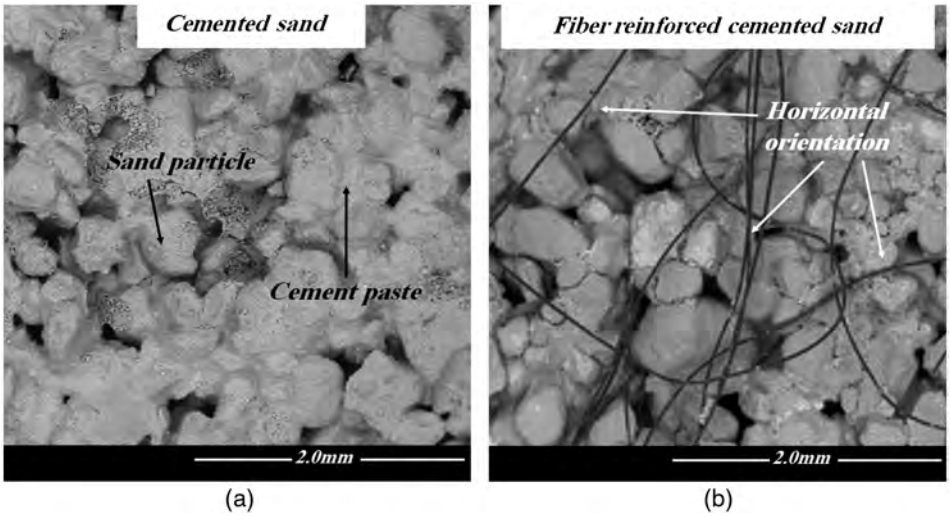

Fig. 10. SEM image: (a) cemented specimens with cement content of 6%; (b) fiber-reinforced cemented sand with 6% cement and 0.6% fiber

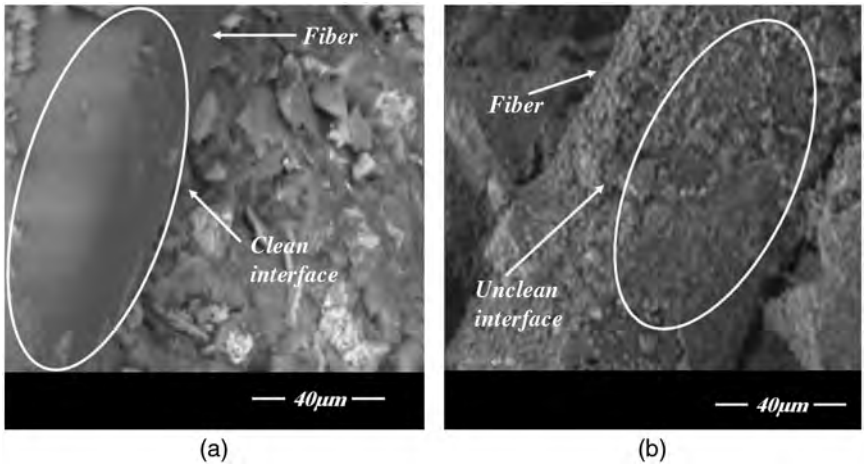

Fig. 11. SEM image: (a) specimen without nanosilica; (b) specimen containing 8% nanosilica

such a procedure produces a preferred near-horizontal orientation of the fibers. Hence, using the moist tamping method for sample preparation leads to having a preferred near-horizontal direction of the fibers, i.e., perpendicular to the ultrasonic pulse's path.

By adding 4 and 8% of nanosilica, the ultrasonic velocity increases, but adding more nanosilica up to 12% would not increase the ultrasonic pulse velocity significantly. The maximum increase in ultrasonic pulse velocity belongs to the sample with 12% nanosilica at the age of 90 days, which is 2.9 km/s, while it is 2.8 km/s for the control sample without nanosilica particles and fiber at the same age. The border layer is a border area between cement paste and the surface of fibers or aggregates or reinforcing elements that plays an important role in durability, strength, and permeability of cement-based composite material. Microstructural properties of the border layer are quite different from the cement paste containing more microcracks and voids. The thickness of the border layer depends on the type of cement agent, water-to-cement ratio, fibers, pozzolanic material, and specimen age.

Fig. 11 shows the SEM images of the cemented sand and fiber surface of the specimens containing 6% cement and 0 and 8% nanosilica. As can be seen from the SEM images, the fiber surface of the sample containing nanosilica particles is completely attached by hydrated products of the cement and sand matrix, which makes the contribution to bond strength and friction between the fiber and cemented sand as compared with the sample without nanosilica particles. In other words, the grooves and pits filled on the fiber surface constituted an interlock and improved the interactions between randomly distributed fiber surface and the cement-stabilized sand particles. If the percentage of nanosilica particles and their spacing is proper, the formation process of calcium hydroxide crystals in the transition zone (border area between cement paste and the surface of fibers or aggregates) decreases, thus the cement paste matrix and transition zone becomes smoother and denser and provides a suitable wave traveling path. Finally, it can be concluded that, regarding hydrated structure of cement thus cement paste with microscale and nanoscale pores, nanosilica can efficiently fill nanopores and increase ultrasonic pulse velocity and unconfined compressive strength of cemented soil. Moreover, nanosilica can increase the bonding strength of cemented sand–fiber interfaces results in an improvement of structural properties of the border layer.

The ultrasonic velocity can be used to estimate the strength of both in situ and precast cemented material. There is no certain relationship between the ultrasonic pulse velocity and the unconfined compressive strength. The module of elasticity is related to the unconfined compressive strength and there is a relationship between the seismic wave velocity, the module of elasticity, and the density of the specimen, so there is a good reason to determine the unconfined compressive strength based on the ultrasonic pulse velocity. Previous studies showed that the relationship between the ultrasonic velocity and unconfined compressive strength can be estimated by the following equation:

$$\mathrm{UCS} = A \cdot e^{(BV)} \tag{8}$$

where UCS = unconfined compressive strength; V = ultrasonic pulse velocity (km/s); and A and B = empirical constants (Ravindrarajah 1997). The function relationships between the ultrasonic velocity and the unconfined compressive strength for all of the fiber reinforcement samples that contain different nanosilica content and cement content regardless of their curing time are defined and shown in Fig. 12.

Scanning Electron Microscope

The microstructure of the samples containing 6% cement and 8% nanosilica for 90 days curing was analyzed by scanning electron microscopic. The middle (central) parts of the samples were taken for investigation of their micromechanical analysis (scanning

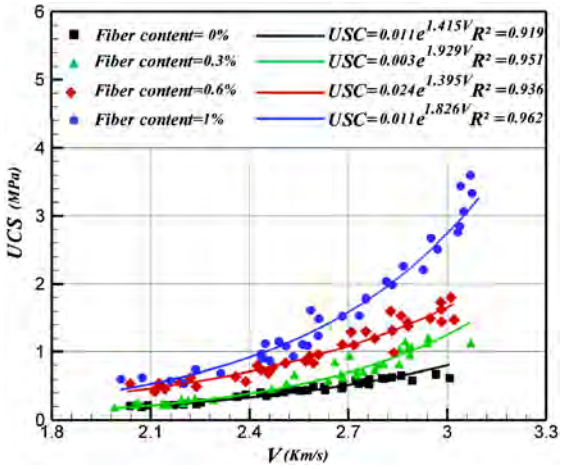

Fig. 12. Relationship between the pulse velocity and compressive strength

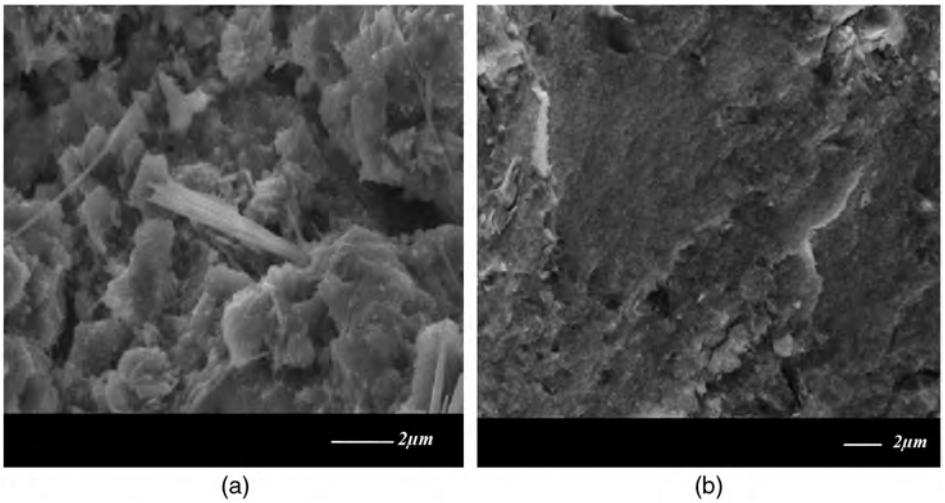

Fig. 13. SEM images of the specimen for 90 days curing: (a) specimen without nanosilica; (b) specimen containing 8% nanosilica

electron microscope image). The surface of the scanning electron microscope sample was cleaned before mounting the sample. The homogenous and uniform structure improved the strength of the soil-cement mixture containing nanosilica compared with the specimen without nanosilica. The SEM micrographs of the samples containing 6% cement and 8% nanosilica for 90 days are shown in Fig. 13. As can be seen from the SEM images, the microstructure of the sample containing nanosilica particles appeared quite dense and compact with relatively less pores and more homogeneous structure as compared with the sample without nanosilica particles. It may reflect the formation of secondary calcium silicate hydrate gel in reactions between the nanosilica particles and the cement. It can be seen that SEM micrograph results confirm the unconfined compressive strength and ultrasonic pulse velocity results and further confirmed that the reactions between the nanosilica particles and the cement products have a positive effect on the behavior of cement-sand mixtures.

X-Ray Diffraction

An X-ray diffraction test was conducted to have a suitable criterion for assessment of pozzolanic activity of nanoparticle. An X-ray diffraction test was conducted on the samples without fibers which have 0 and 8% nanosilica and 6% cement content at the age of 90 days. Fig. 14 shows the XRD graphs of samples with 6% cement and without nanosilica and with 8% nanosilica for 90 days curing. The presence of the calcium silicate hydrate phase could be confirmed by the presence of peak at $2\theta = 29°$ and peaks at $2\theta = 18°$ and $2\theta = 33°$, which are related to the calcium hydroxide phase (Bahmani et al. 2014). As seen in Fig. 14, the addition of nanosilica to the matrix cemented sand reduced the intensity of the peaks attributable to the formation of calcium hydroxide and increased the intensity of the peaks attributable to the formation of calcium silicate hydrate. This result indicates that pozzolanic activity of nanosilica particles efficiently reduced calcium hydroxide formation in the cemented sand samples. The reduction in calcium hydroxide formation and increase in the amount of calcium hydroxide makes the cement past matrix and transmission zone more uniform, compact, and homogeneous. The results from the X-ray diffraction test may well explain the increased unconfined compressive strength and ultrasonic pulse velocity of samples containing nanosilica.

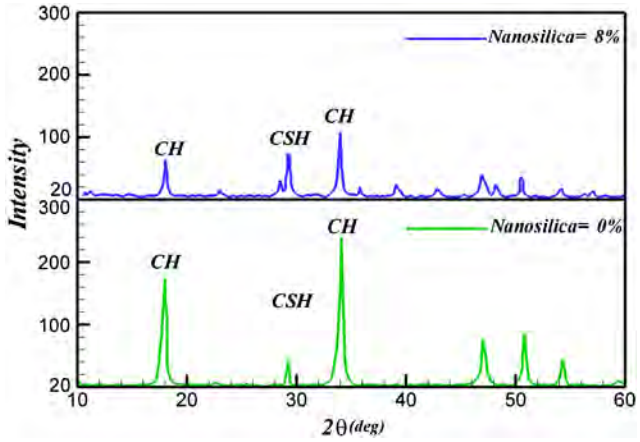

Fig. 14. XRD patterns of the concrete samples containing 0 and 8% nanosilica

Conclusion

This research evaluated the impacts of nanosilica particles and randomly distributed fibers on the mechanical properties and ultrasonic pulse velocity of cemented sand. Other limitations linked to cement agent, soil, nanoparticle, and fiber cement were investigated. Further research is still necessary to check if such a result might be spread to other fibers (e.g., nylon, glass, polyester, and polypropylene), nanoparticles (nanoclay, carbon nanotube, nano alumina, nano copper), soils (e.g., silt, loess, and clay), as well as to other cement agents, such as lime, cement kiln dust, lime fly ash, gypsum plaster, and calcite cement. The obtained results can be summarized as follows:

- The inclusion of portland cement to the sandy soil increased the secant modules of elasticity and compression strength and changed the sand behavior to a noticeably more brittle behavior.
- Inclusion of randomly distributed fiber causes an increase in the energy absorption capacity and compression strength in the cement-stabilized soil. In addition, the secant modulus of elasticity decreases with increasing fiber content.
- When the percentage of nanosilica is increased up to 8% of the cement agent weight in the samples, there was a significant increase in ultrasonic pulse velocity. This was due to filling and

pozzolanic effects of nanosilica particles in transmission zone and cement paste matrix. Moreover, the older the specimen is the higher the ultrasonic pulse velocity will be. In addition, the proposed equation by Ravindrarajah (1997), which was an exponential relationship between unconfined compressive strength and ultrasonic velocity in concrete, has been adapted for the fiber-reinforced cemented sand containing nanoscilica.

- It seems that adding 0.3% fiber increases the ultrasonic velocity in almost all of the specimens for all of the curing times, but adding more fiber (0.6 and 1%) decreases the ultrasonic pulse velocity. Moreover, the ultrasonic pulse velocity increases with increase of the curing time.
- The obtained results from the scanning electron microscopic indicated that the surface of the specimen containing the nanosilica was more uniform and compact than that without nanosilica, which causes improvement of the mechanical properties of the cemented sand.
- Results of X-ray diffraction graphs and its calcium hydroxide peaks reveal that the addition of nanosilica particles to the matrix cemented sand reduced the intensity of the peaks that are attributable to the formation of calcium hydroxide and nanosilica's pozzolanic activity.

References

ASTM. (2010a). "Standard test method for measurement of soil suction using filter paper." *ASTM D5298*, West Conshohocken, PA.

ASTM. (2010b). "Standard test method for unconfined compressive strength of cohesive soil." *ASTM D2166*, West Conshohocken, PA.

ASTM. (2010c). "Standard test methods for laboratory compaction characteristics of soil using standard effort." *ASTM D698*, West Conshohocken, PA.

Ateş, A. (2016). "Mechanical properties of sandy soils reinforced with cement and randomly distributed glass fibers (GRC)." *Compos. Part B*, 96, 295–304.

Bahadori, H., and Hosseini, P. (2012). "Reduction of cement consumption by the aid of silica nano-particles (investigation on concrete properties)." *J. Civ. Eng. Manage.*, 18(3), 416–425.

Bahmani, S. H., Huat, B. B. K., Asadi, A., and Farzadnia, N. (2014). "Stabilization of residual soil using SiO2 nanoparticles and cement." *Constr. Build. Mater.*, 64, 350–359.

Beigi, M. H., Berenjian, J., Lotfi, O. O., Sadeghi Nik, A., and Nikbin, I. (2013). "An experimental survey on combined effects of fibers and nanosilica on the mechanical, rheological, and durability properties of self-compacting concrete." *Mater. Des.*, 50, 1019–1029.

Chang, T. S., and Woods, R. D. (1992). "Effect of particle contact bond on shear modulus." *J. Geotech. Eng.*, 10.1061/(ASCE)0733-9410(1992)118:8(1216), 1216–1233.

Choobbasti, A. J., Tavakoli, H., and Kutanaei, S. S. (2014). "Modeling and optimization of a trench layer location around a pipeline using artificial neural networks and particle swarm optimization algorithm." *Tunnelling Underground Space Technol.*, 40, 192–202.

Choobbasti, A. J., Vafaei, A., and Kutanaei, S. S. (2015). "Mechanical properties of sandy soil improved with cement and nanosilica." *Open Eng.*, 5(1), 111–116.

Clough, G. W., Sitar, N., Bachus, R. C., and Rad, N. S. (1981). "Cemented sands under static loading." *J. Geotech. Eng. Div.*, 107(6), 799–817.

Consoli, N. C., Bassani, M. A. A., and Festugato, L. (2010). "Effect of fiber-reinforcement on the shear strength of cemented soils." *Geotext. Geomembr.*, 28(4), 344–351.

Consoli, N. C., Cruz, R. C., Da Fonsea, A. V., and Coop, M. R. (2012). "Influence of cement-voids ratio on stress-dilatancy behavior of artificially cemented sand." *J. Geotech. Geoenviron. Eng.*, 10.1061/(ASCE)GT.1943-5606.0000565, 100–109.

Consoli, N. C., Montardo, J. P., Donato, M., and Prietto, P. D. M. (2004). "Effect of material properties on the behaviour of sand-cement–fibre composites." *Ground Improv.*, 8(2), 77–90.

Consoli, N. C., Rotta, G. V., and Prietto, P. D. M. (2000). "The influence of curing under stress on the triaxial response of cemented soils." *Géotechnique*, 50(1), 99–105.

Dehghan, A., and Hamidi, A. (2016). "Triaxial shear behaviour of sand-gravel mixtures reinforced with cement and fibre." *Int. J. Geotech. Eng.*, 1–11.

Ghasabkolaei, N., Janalizadeh, A., Jahanshahi, M., Roshan, N., and Ghasemi, S. E. (2016). "Physical and geotechnical properties of cement-treated clayey soil using silica nanoparticles: An experimental study." *Eur. Phys. J. Plus*, 131(5), 1–11.

Ibraim, E., Diambra, A., Russell, A. R., and Muir Wood, D. (2012). "Assessment of laboratory sample preparation for fibre reinforced sands." *Geotext. Geomembr.*, 34, 69–79.

Kutanaei, S. S., and Choobbasti, A. J. (2015a). "Prediction of combined effects of fibers and cement on the mechanical properties of sand using particle swarm optimization algorithm." *J. Adhes. Sci. Technol.*, 29(6), 487–501.

Kutanaei, S. S., and Choobbasti, A. J. (2015b). "Triaxial behavior of fiber reinforced cemented sand." *J. Adhes. Sci. Technol.*, 30(6), 579–593.

Kutanaei, S. S., and Choobbasti, A. J. (2016). "Experimental study of combined effects of fibers and nanosilica on mechanical properties of cemented sand." *J. Mater. Civ. Eng.*, 10.1061/(ASCE)MT.1943-5533.0001521, 06016001.

Ladd, R. S. (1978). "Preparing test specimens using undercompaction." *Geotech. Test. J.*, 1(1), 16–23.

Li, G. (2004). "Properties of high-volume fly ash concrete incorporating nano-SiO2." *Cem. Concr. Res.*, 34(6), 1043–1049.

Li, H., Xiao, H. G., Yuan, J., and Ou, J. (2005). "Microstructure of cement mortar with nanoparticles." *Compos. Part B*, 35(2), 185–189.

Li, H., Zhang, M. H., and Ou, J. P. (2006). "Abrasion resistance of concrete containing nanoparticles for pavement." *Wear*, 260(11–12), 1262–1266.

Luo, H. L., Hsiao, D. H., and Lin, C. K. (2012). "Cohesive soil stabilized using sewage sludge ash/cement and nano aluminum oxide." *Int. J. Transp. Sci. Technol.*, 1(1), 83–100.

Maher, M. H., and Ho, Y. C. (1993). "Behavior of fiber-reinforced cemented sand under static and cyclic loads." *Geotech. Test. J.*, 16(3), 330–338.

Ravindrarajah, R. (1997). "Strength evaluation of high-strength concrete by ultrasonic pulse velocity method." *NDT & E Int.*, 30(4), 262.

Taha, M. R. (2009). "Geotechnical properties of soil-ball milled soil mixtures." *Proc., 3rd Symp. on Nanotechnology in Construction*, Springer, Berlin, 377–382.

Tang, C., Shi, B., Gao, W., Chen, F., and Cai, Y. (2007). "Strength and mechanical behavior of short polypropylene fiber reinforced and cement stabilized clayey soil." *Geotext. Geomembr.*, 25(3), 194–202.

Tang, C., Wang, D., Cui, Y., Shi, B., and Li, J. (2016). "Tensile strength of fiber-reinforced soil." *J. Mater. Civ. Eng.*, 10.1061/(ASCE)MT.1943-5533.0001546, 04016031.

Tavakoli, H. R., Omran, O. L., Kutanaei, S. S., and Shiade, M. F. (2014a). "Prediction of energy absorption capability in fiber reinforced self-compacting concrete containing nano-silica particles using artificial neural network." *Lat. Am. J. Solids Struct.*, 11(6), 966–979.

Tavakoli, H. R., Omran, O. L., Shiade, M. F., and Kutanaei, S. S. (2014b). "Prediction of combined effects of fibers and nano-silica on the mechanical properties of self-compacting concrete using artificial neural network." *Lat. Am. J. Solids Struct.*, 11(11), 1906–1923.

Wood, M. D., Russell, A. R., Ibraim, E., and Diambra, A. (2007). "Determination of fibre orientation distribution in reinforced sands." *Geotechnique*, 57(7), 623–628.